Snapshot phase shift fringe projection 3D surface measurement

Article *in* Optics Express · January 2015

DOI: 10.1364/OE.23.000667

CITATIONS
11

READS
279

3 authors, including:

Zhenyue Chen
University of Zurich
19 PUBLICATIONS **129** CITATIONS
SEE PROFILE

Xia Wang
Beijing Institute of Technology
122 PUBLICATIONS **503** CITATIONS
SEE PROFILE

Snapshot phase shift fringe projection 3D surface measurement

Zhenyue Chen,[1,2] Xia Wang,[2] and Rongguang Liang[1,*]

[1]*College of Optical Sciences, University of Arizona, Tucson, Arizona 85721, USA*
[2]*Beijing Institute of Technology, Key Laboratory of Photoelectronic Imaging Technology and System of Ministry of Education of China, School of Optoelectronics, Beijing 100081, China*
[*]*rliang@optics.arizona.edu*

Abstract: We propose a novel snapshot phase shift fringe projection three-dimensional (3D) surface measurement method using polarization-coded light illumination and polarization camera. The light from the light source is split into two beams, one is left circularly polarized and the other is right circularly polarized, to illuminate the object simultaneously. A four-channel division of focal plane (DoFP) polarization camera is employed to capture the light reflected from the object surface. Four images with a phase shift of $\pi/2$ are extracted from the snapshot image and then analyzed to reconstruct a 3D object surface. The proposed method is the first snapshot phase shift fringe projection approach for 3D surface imaging. It is insensitive to motion and has the potential for ultrafast 3D surface imaging.

OCIS codes: (120.6650) Surface measurements, figure; (110.6880) Three-dimensional image acquisition; (150.6910) Three-dimensional sensing; (120.5050) Phase measurement.

References and links

1. J. Geng, "Structured-light 3D surface imaging: a tutorial," Adv. Opt. Photonics **3**(2), 128–160 (2011).
2. X. Su and W. Chen, "Fourier transform profilometry: a review," Opt. Lasers Eng. **35**(5), 263–284 (2001).
3. J. Geng, "Rainbow three-dimensional camera: new concept of high-speed three-dimensional vision systems," Opt. Eng. **35**(2), 376–383 (1996).
4. P. S. Huang, C. Zhang, and F. Chiang, "High-speed 3-D shape measurement based on digital fringe projection," Opt. Eng. **42**(1), 163–168 (2003).
5. S. Zhang, "Recent progresses on real-time 3-D shape measurement using digital fringe projection techniques," Opt. Lasers Eng. **48**(2), 149–158 (2010).
6. S. Lei and S. Zhang, "Digital sinusoidal fringe generation: defocusing binary patterns VS focusing sinusoidal patterns," Opt. Lasers Eng. **48**(5), 561–569 (2010).
7. B. Li, Y. Wang, J. Dai, W. Lohry, and S. Zhang, "Some recent advances on superfast 3D shape measurement with digital binary defocusing techniques," Opt. Lasers Eng. **54**, 236–246 (2014).
8. S. Heist, M. Sieler, A. Breitbarth, P. Kühmstedt, and G. Notni, "High-speed 3D shape measurement using array projection," Proc. SPIE **8788**, 878815 (2013).
9. M. Schaffer, M. Grosse, B. Harendt, and R. Kowarschik, "High-speed three-dimensional shape measurements of objects with laser speckles and acousto-optical deflection," Opt. Lett. **36**(16), 3097–3099 (2011).
10. M. Grosse, M. Schaffer, B. Harendt, and R. Kowarschik, "Fast data acquisition for three-dimensional shape measurement using fixed-pattern projection and temporal coding," Opt. Eng. **50**(10), 100503 (2011).
11. M. Schaffer, M. Große, B. Harendt, and R. Kowarschik, "Coherent two-beam interference fringe projection for highspeed three-dimensional shape measurements," Appl. Opt. **52**(11), 2306–2311 (2013).
12. B. Salahieh, Z. Chen, J. J. Rodriguez, and R. Liang, "Multi-polarization fringe projection imaging for high dynamic range objects," Opt. Express **22**(8), 10064–10071 (2014).
13. B. M. Ratliff, C. F. LaCasse, and J. S. Tyo, "Interpolation strategies for reducing IFOV artifacts in microgrid polarimeter imagery," Opt. Express **17**(11), 9112–9125 (2009).

1. Introduction

A number of optical techniques for three-dimensional (3D) surface measurement using phase shift fringe projection method have been developed and are currently commercially available. Generally, they can be classified into either sequential (multiple-shot) or single-shot categories [1]. If the target 3D object is stationary and the application does not impose

#226296 - $15.00 USD Received 5 Nov 2014; revised 20 Dec 2014; accepted 31 Dec 2014; published 12 Jan 2015

stringent constraints on the acquisition time, multiple-shot techniques are often used because they provide more reliable and accurate results. For moving objects, single-shot techniques are desired to acquire 3D surface images. Current single-shot techniques, such as the Fourier transform method, do not provide sufficient measurement accuracy [2]. The rainbow three dimensional camera has the snapshot ability to achieve 3D surface measurement with a color-coded single pattern [3]; the limitations of this approach includes color cross-talk in the sensor and distorted color information from the color object. Digital fringe projection phase shifting technique is a full-field and high-resolution multi-shot 3D shape measurement method; the measurement of fast moving or changing objects is difficult because at least three fringe patterns are required [4]. Recent advances in superfast 3D measurement have achieved high speed measurement up to kHz. One approach is to use a high-speed camera and digital binary pattern projection by the digital light processing projectors [5–7]. Heist et al. presented the concepts and a realized setup of a 3D array projector with frame rate up to 100 kHz [8]. Schaffer et al. used laser speckles as projected patterns which were switched using an acousto-optical deflector to achieve high speed, dense 3D measurement [9]. Grosse et al. demonstrated a 3D measurement method with acquisition rate more than 700 with stereo-photogrammetry and slide-projector [10]. Schaffer et al. utilized two-beam interference Fizeau fringes for 3D shape measurement [11]. With an acousto-optical deflector the phase shift rate is up to 200,000 Hz.

In this paper, for the first time we propose a novel snapshot phase shift fringe projection 3D surface measurement method. Instead of projecting and capturing at least three phase shifted fringe patterns, we illuminate the object with two orthogonal circularly polarized beams. A four-channel division of focal plane (DoFP) polarization camera [12] is employed to capture the reflected light from the object surface. Four phase shifted images with a phase shift of $\pi/2$ are extracted from DoFP polarization camera to reconstruct the 3D surface shape.

2. Principle and experimental setup

To demonstrate the concept, we build the experimental setup as shown in Fig. 1. There are a number of methods to generate two circularly polarized beams from a single light source, in this study we use a simple, but easily implemented, beam splitting method. The laser beam from a 650 nm diode laser is split into two beams with orthogonal polarizations using a polarizing beam splitter and then combined together using another polarizing beam splitter. Two polarized beams are converted to orthogonal circularly polarized beams by a quarter wave plate. A low power microscope objective is employed to generate divergent illumination beams to cover the object surface. Two linear polarizers are added into the setup to improve the linear polarization degrees of two beams. A liquid crystal diffuser is also used to reduce the coherence length of the laser light. The fringe pitch can be adjusted by tilting one of the beams. A four-channel DoFP polarization camera as shown in Fig. 1 is employed to capture the reflected light from the object surface. The camera has a resolution of 1608x1208 pixels and has a maximum frame rate of 35 fps at full resolution.

#226296 - $15.00 USD Received 5 Nov 2014; revised 20 Dec 2014; accepted 31 Dec 2014; published 12 Jan 2015

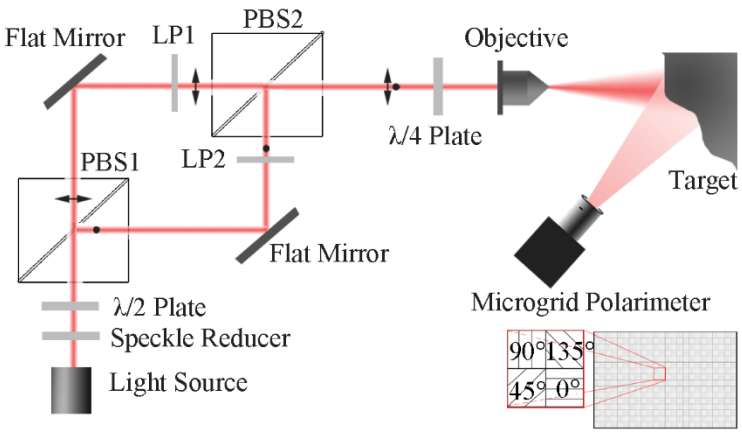

Fig. 1. Experimental setup. PBS1 and PBS2 - first and second polarization beam splitters, LP1 and LP2 - first and second linear polarizers.

Assume that a monochromatic plane wave in any state of polarization is incident on the first PBS. The Jones vector E_{in} with normalized intensity for the incident electric field is described by

$$E_{in} = \begin{bmatrix} E_x \\ E_y \end{bmatrix} = \begin{bmatrix} \cos\alpha \\ e^{i\delta}\sin a \end{bmatrix}, \tag{1}$$

where α is an auxiliary angle for the polarization ellipse and δ is the initial phase difference between E_x and E_y. The light is then split into two beams with orthogonal polarization states. After combination at the second PBS, the electric field is the same as E_{in}. The Jones matrix of a quarter wave plate with an orientation angle of 45 degrees is described by

$$QWLR[\frac{\pi}{2}, 45^\circ] = \frac{1}{\sqrt{2}}\begin{bmatrix} 1 & -i \\ -i & 1 \end{bmatrix}. \tag{2}$$

The electric field after passing through the quarter wave plate is

$$E = \frac{1}{\sqrt{2}}\begin{bmatrix} \cos\alpha - ie^{i\delta}\sin\alpha \\ -i\cos\alpha + e^{i\delta}\sin\alpha \end{bmatrix}. \tag{3}$$

When a linear polarizer at an angle β with respect to the x-axis is placed after the quarter wave plate, the two orthogonal circularly polarized beams interfere. The intensity of the light after passing through a linear polarizer is

$$I = \frac{1}{2}[1 + \sin(2\alpha)\sin(\delta + 2\beta)]. \tag{4}$$

Equation (4) shows that a linear polarizer oriented at an angle β introduces a phase shift change of 2β. This implies that we can obtain images with variable phase shifts by rotating the linear polarizer. By using the DoFP camera which has four different linear polarization orientations, i.e., 0, π/4, π/2 and 3π/4, four images with phase shift of 0, π/2, π and 3π/2 are acquired in a single shot.

3. Experimental results

To verify the proposed method, the fringe pattern from the microscope objective is imaged directly onto the DoFP sensor with the imaging lens from the DoFP camera removed. Figure 2(a) shows the raw image from the DoFP polarization camera. Figures 2(b)-2(e) show the four

#226296 - $15.00 USD Received 5 Nov 2014; revised 20 Dec 2014; accepted 31 Dec 2014; published 12 Jan 2015

phase shifted images extracted from the raw image. Figure 2(f) shows the intensity distribution in false color after the four phase shifted images are combined and transferred to 16 bit. Figure 2(f) shows that the intensity distribution is not uniform with stripe patterns, indicating that the fringe patterns are not ideal. Figure 2(g) shows the line profiles along the image width of the four phase shifted images as shown in Figs. 2(b)-2(e). The intensities of the four polarization channels are not the same, which is one of the causes for the stripe patterns in Fig. 2(f). This is discussed in more detail in the next section.

Figure 3 shows the experimental results using the polarization-coded structured illumination to measure the shape of a machined aluminum part. The measured area is around 2.5x2.5 cm^2. The peak height is 3.2 mm. Figures 3(a)-3(d) are the four phase shifted images; Fig. 3(e) shows the image of the aluminum plate; Fig. 3(f) shows the measured surface shape plotted in 3D mesh rendering. This experiment shows that the proposed method is able to capture four phase shifted images to measure 3D surface shape in a snapshot.

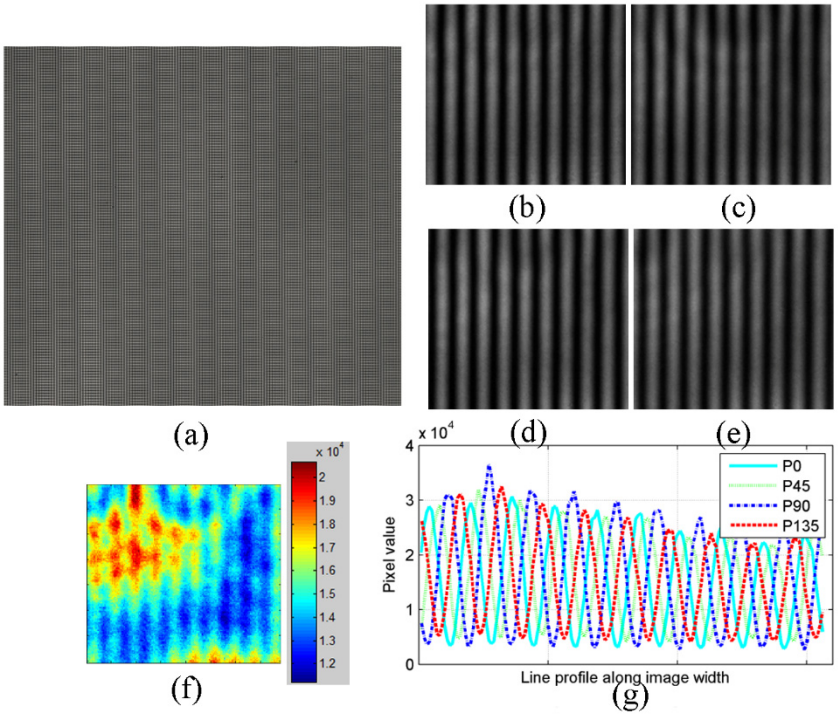

Fig. 2. Experiment results when the polarization camera without an imaging lens is placed at the focal plane of the microscope objective. (a) Raw image, (b) P0 image, (c) P45 image with phase shift of $\pi/2$, (d) P90 image with phase shift of π, (e) P135 image with phase shift of $3\pi/2$, (f) intensity distribution in false color, and (g) line profile of the four phase shift images.

#226296 - $15.00 USD Received 5 Nov 2014; revised 20 Dec 2014; accepted 31 Dec 2014; published 12 Jan 2015

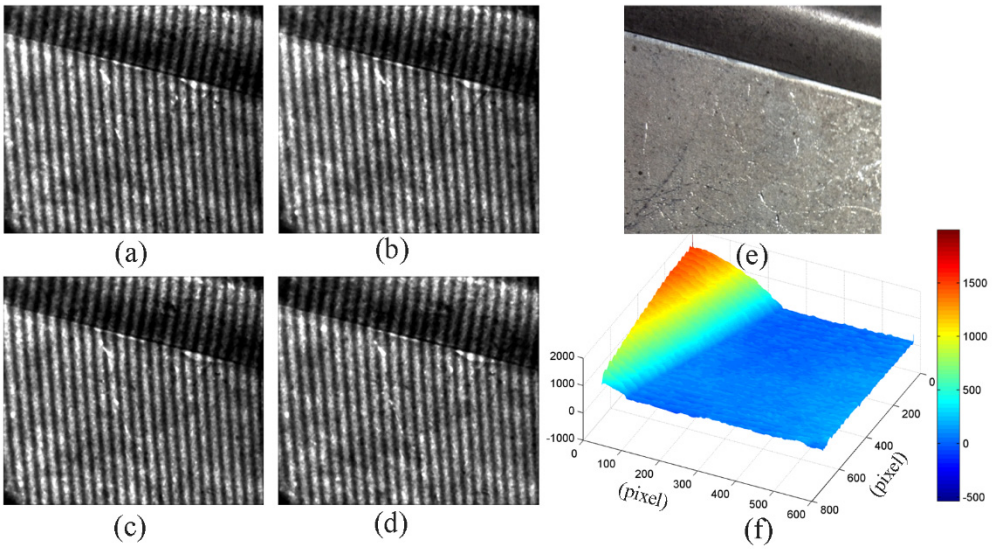

Fig. 3. 3D surface measurement of a machined aluminum part. (a) - (d) phase shifted images, (e) image of the aluminum part, and (f) mesh rendering of 3D surface shape. The unit of x, y axis is pixel and the unit of z axis is 1.

4. Error analysis

As shown in Figs. 2(f) and 2(g), the fringe patterns are not ideal with stripe patterns. There are two possible reasons for this phenomenon. First, the two beams are not ideal circularly polarized light, which could be caused by (1) the wavelength mismatch between the laser and the quarter wave plate and/or (2) the orientation error of the quarter wave plate with respect to the orientation of the linear polarized light. In our experiment, the light source is 650 nm diode laser, the center wavelength of the quarter wave plate is 670 nm. The effect of the wavelength mismatch of the quarter wave plate is simulated. The retardance of the quarter wave plate for the incident light with central wavelength at 650 nm is 0.515π. With horizontally and vertically polarized incident light, the Jones vectors are

$$E_H = 10\begin{bmatrix}1\\0\end{bmatrix}, E_V = 6\begin{bmatrix}0\\1\end{bmatrix}. \tag{5}$$

Here we set the amplitude of the two beams as 10 and 6 respectively, to simulate an intensity difference between two beams. The orientation of the quarter wave plate is oriented at 45 degrees to the horizontal. After going through the quarter wave plate, the electrical field of the non-ideal right and left circularly polarized light are

$$E_{RC} = 10\begin{bmatrix}0.7290i\\0.6846\end{bmatrix}, E_{LC} = 6\begin{bmatrix}0.6846\\0.7290i\end{bmatrix}, \tag{6}$$

When reaching the focal plane array, the two beams interfere. Figure 4(a) shows the line profiles of the four phase shifted images. Note that the intensities of four images are slightly different. Figure 4(b) is the combined image of four channels. The intensity distribution is uniform. It means that the wavelength mismatch in the experiment is negligible. When the angle of linear polarization (AoLP) of the incident light deviates slightly from horizontally and vertically polarized light, for instance, AoLP being 5°and 83°, the corresponding E_H and E_V is

#226296 - $15.00 USD Received 5 Nov 2014; revised 20 Dec 2014; accepted 31 Dec 2014; published 12 Jan 2015

$$E_H = 10\begin{bmatrix}0.996\\0.094\end{bmatrix}, E_V = 6\begin{bmatrix}0.125\\0.992\end{bmatrix}. \quad (7)$$

The line profiles of the four phase shifted images are shown in Fig. 4(c). Note that there are both intensity variations and small phase shift errors in different polarization channels. Consequently, the combination of the four images has severe stripe patterns as shown in Fig. 4(d). Thus, we conclude that the stripe pattern is sensitive to the orientation error between the quarter wave plate and the linear polarizers.

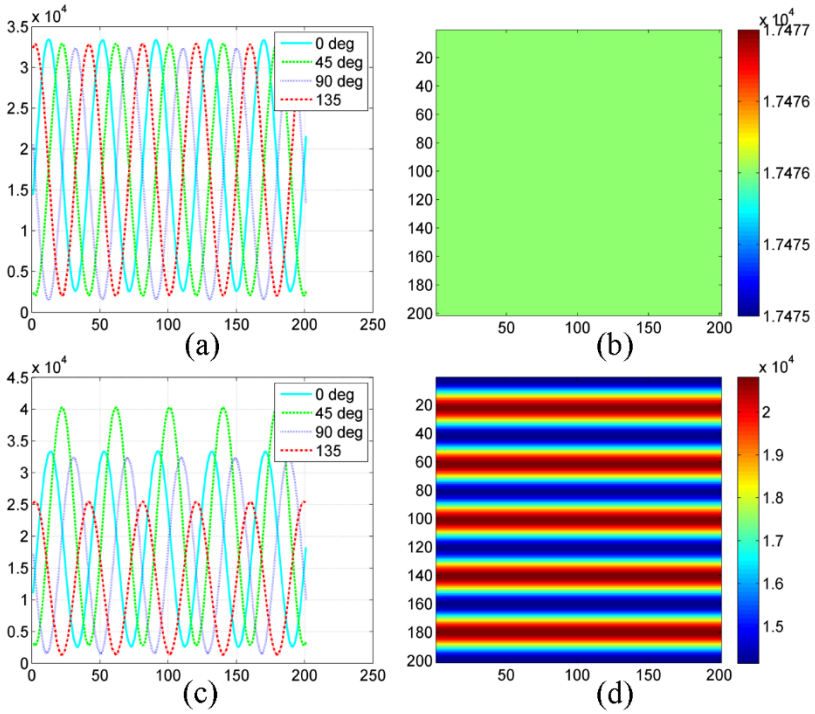

Fig. 4. Simulation results of wavelength mismatch and orientation error. (a) Line profile of the four phase shifted images with wavelength mismatch. (b) Combination of the four images in (a). (c) Line profile of the four phase shifted images with wavelength mismatch and orientation error. (d) Combination of the four images in (c).

Also, the different responses of the four polarization channels of the camera causes intensity variations. The instantaneous field-of-view (IFOV) error of the camera contributes to the stripe pattern [13]. The four phase shifted images represented by the profiles in Fig. 4(a) are downsampled to acquire the microgrid polarization image. Then interpolation methods are employed to minimize the IFOV error. Figure 5 shows the simulation results of IFOV error before and after interpolation. In Fig. 5(a) we investigate the relationship between IFOV error and spatial frequency by generating a series of targets with spatially varying intensity sinusoidal patterns. The root-mean-square error (RMSE) of intensity without and with different interpolation methods are shown. Figure 5(a) shows the combination of the four phase shifted images after downsampling. Note that due to the IFOV error, the stripe pattern is obviously perceived. Figure 5(c) shows the combination image of the four phase shifted images after "spline" interpolation. Note that with "spline" interpolation, the IFOV error is minimized. We have developed a calibration method to minimize the fixed pattern noise and photon response non-uniformity as well as IFOV error.

#226296 - $15.00 USD Received 5 Nov 2014; revised 20 Dec 2014; accepted 31 Dec 2014; published 12 Jan 2015

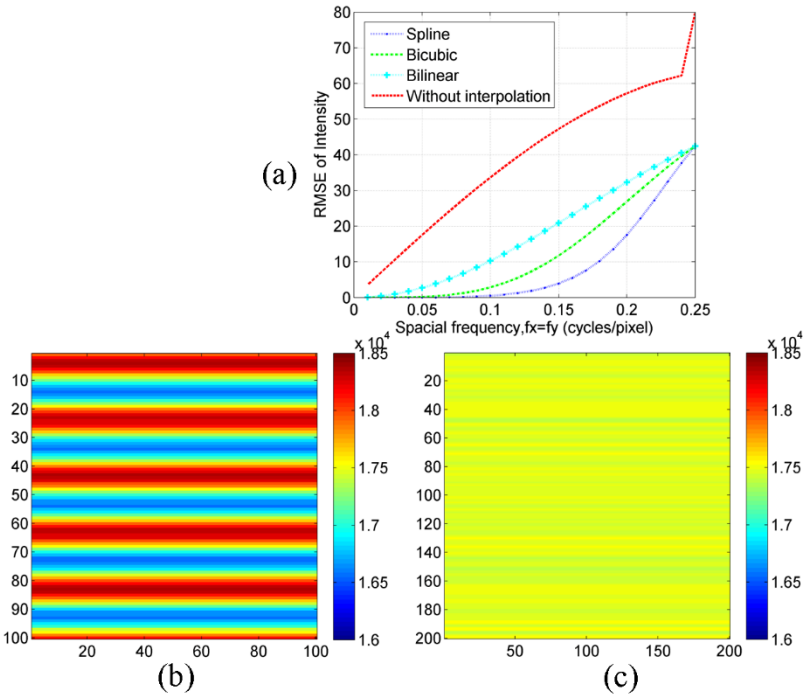

Fig. 5. IFOV error before and after interpolation. (a) RMSE of intensity with and without interpolation method. (b) Combination of four phase shifted images without interpolation. (c) Combination of the four phase shifted images with "spline" interpolation.

5. Conclusions

In summary, for the first time we have demonstrated a novel snapshot phase shift fringe projection 3D surface shape measurement using circularly polarized light illumination and polarization camera. This method is able to measure moving objects or objects with varying shapes in high speed using fast polarization cameras, which can be built from fast CCD or CMOS cameras with pixelated polarizer arrays. One potential issue is the impact of the depolarization from the object. It reduces the image contrast and may introduce the measurement error. Another issue is speckle when a laser is used as the light source. We are in the progress of addressing the speckle by using a LED as the light source because it has a much shorter coherence length. In the meantime, we are investigating the impact of depolarization and methods to minimize the potential impact.

Acknowledgments

This work is partially supported by a grant of the China Scholarship Council (No. 201306030018). We would also like to thank Shaun Pacheco for manuscript revision suggestions.

#226296 - $15.00 USD Received 5 Nov 2014; revised 20 Dec 2014; accepted 31 Dec 2014; published 12 Jan 2015